International Aerospace CFD Conference
(Paris, June 18 – 19 2007)

Ice Accretion Prediction on Aerodynamic Bodies

C. R. Maliska
A. F. C. da Silva
R. A. Silveira
C. N. Donatti
G. L. Bridi

SINMEC - Computational Fluid Dynamics Lab
Mechanical Engineering Department
Federal University of Santa Catarina
Florianópolis, SC, Brazil

ABSTRACT: The prediction of ice accretion on aerodynamic profiles during flight is required for the design of the anti-icing system as well as for the determination of the aerodynamic degradation in the presence of ice layers. To perform the prediction of the ice accretion, knowledge of the flow around the aerodynamic body coupled with a thermodynamic model for the calculation of the ice growth is required. This coupling, if not handled carefully, will result in complex and time consuming codes, not appropriate for engineering applications. The goal of this study is to develop a 2D thermodynamic model for the ice accretion coupled with a 2D external flow solution. The strategy is to apply the developed model to several 2D slices obtained from cutting the 3D geometry and the respective 3D external flow solution. The thermodynamic model follows the pioneering ideas of Messinger [1] and considers the mass and energy balances for control volumes located over the surface, so that the temperature and the freezing rate can be computed. The mass balance accounts for the impinging water, evaporation, runback and freezing, while the energy balance considers the air and water kinetic heating, evaporative cooling, convection, conduction, sensible energy and latent heat due to phase change. Impinging water fluxes, heat transfer coefficient, pressure and skin friction are obtained from the external flow solution. The water droplet trajectories, required for the collection efficiency, can be calculated by two approaches. The first one uses a Lagrangian formulation for the determination of the impingement positions of the water droplets at the body surface. The second solves the two-phase (air-water) flow around the body by using a two-fluid model. In this work the commercial CFD software CFX was used for this purpose. The developed computational tool was employed for the prediction of ice accretion for different aerodynamic profiles in several flying conditions. The results were compared with available experimental data and with numerical results from other codes.

Keywords: Ice accretion, collection efficiency, Lagrangian formulation, two-fluid model, lift degradation

INTRODUCTION

This paper presents a numerical procedure for predicting ice shapes accreted on the leading edge of aerodynamic profiles. Special attention is given to the determination of the collection efficiency by solving the two-phase air/water flow with the CFX package. It is common to use the Lagrangian formulation for the collection efficiency calculation, but comparisons performed show that more general methods can be devised for predicting ice accretion in complex geometries. Several works use the Lagrangian methodology, as in the codes Lewice (Wright, 1995), Canice (Morency et al., 1999) and Trajice2 (Gent, 1994), and in the work of Silveira and Maliska (2001). All these models use boundary layer integration for thermal and viscous effects and droplet trajectory calculation for collection efficiency. This methodology takes advantage for being relatively simple and fast. However, for complex geometries, especially for 3D cases, the "particle-tracking" approach becomes difficult to implement and is computationally very expensive. In addition, the potential flow assumption is limited to low Mach numbers and low angles of attack.

To deal with complex geometries and flow conditions, the Eulerian-Eulerian approach has been successfully applied for icing analysis. The Fensap-Ice Code (Bourgault et al., 2000), using finite elements, computes the two-phase flow by assuming that the droplets do not affect the airflow, therefore, considering them as a passive scalar. The work of Naterer (2002), for ice accretion on electricity transmission lines, considers a full multiphase flow, that is, the water droplets are also assumed to affect the airflow. In this case, the same equations solved for the airflow are also solved for the water droplets (disperse phase). Silveira et al. (2003) used the two-fluid model available in the CFX commercial code to solve the external aerodynamics flow problem.

External flow results, like collection efficiency, heat transfer coefficient, wall shear stress and pressure distribution at the wall, in addition to the environmental conditions, such as velocity, static pressure and static temperature, are the input data for the thermodynamic model. Basically, it consists of carrying out a coupled mass-energy balance in each control volume defined over the surface of the geometry, so that the freezing rate is computed and the ice thickness is obtained for each finite segment which also defines the surface. This approach is used in Wright (1995) and Silveira and Maliska (2001).

EXTERNAL FLOW CALCULATION

THE COLLECTION EFFICIENCY DEFINITION

The determination of the collection efficiency requires the knowledge of the flow trajectories. The collection efficiency is define as the ratio between the particle trajectories reaching the wall and the free-stream water fluxes, which can be expressed as

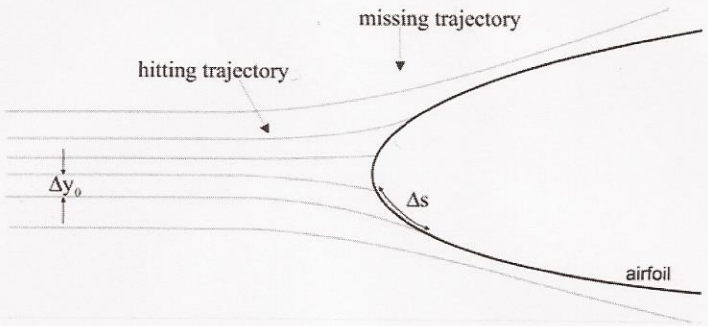

Fig. 1: Droplets trajectories near the airfoil leading edge.

$$\beta = \frac{\dot{m}''_{wall}}{\dot{m}''_{\infty}} \tag{1}$$

Since the mass flow is constant between two streamlines, one can write

$$\dot{m}_{\infty} = \dot{m}_{wall} \tag{2}$$

In terms of fluxes, the above relation can be written, according to Fig.1, as

$$\dot{m}''_{\infty} \Delta y_0 = \dot{m}''_{wall} \Delta s \tag{1}$$

with the local collection efficiency given by

$$\beta = \frac{\Delta y_0}{\Delta s} \tag{2}$$

THE EULERIAN-EULERIAN APPROACH

In this kind of methodology both air and water droplets are treated as continuum phases, and the transport equations are solved for the two "fluids".

The concept of phase volume fraction is introduced, defined as the portion of a control volume "filled" by that phase, according to

$$r_i = \frac{V_i}{V} \tag{3}$$

where V_i is the volume occupied by phase i, with i = 1 for the air (continuum phase) and i = 2 for the water (disperse phase). In this model, the water droplets also affect the airflow, whereas for the work of Bourgault et al. (2000) and for the Lagrangean approach, only the influence of the airflow on the water droplets is considered.

By using this concept, the continuity equation for the phase i is written as

$$\frac{\partial(r_i \rho_i)}{\partial t} + \vec{\nabla} \cdot \left(\rho_i r_i \overrightarrow{U_i}\right) = 0 \tag{4}$$

The momentum equation, considering the Reynolds averaging for turbulence, is also solved for each phase, and is given by

$$\frac{\partial\left(r_i \rho_i \overrightarrow{U_i}\right)}{\partial t} + \vec{\nabla} \cdot \left(r_i \rho_i \overrightarrow{U_i}\,\overrightarrow{U_i}\right) = -r_i \vec{\nabla} p_i' + \vec{\nabla} \cdot \left\{ r_i \mu_{eff,i} \left[\vec{\nabla}\overrightarrow{U_i} + \left(\vec{\nabla}\overrightarrow{U_i}\right)^T \right] \right\} + \overrightarrow{S_i} + \overrightarrow{M_i} \tag{7}$$

in which p_i' and $\mu_{eff,i}$ are the pressure and effective viscosity of the phase i, respectively. S_i is related to momentum sources due to external forces and M_i represents the interfacial forces. Interfacial forces encompass virtual mass, drag, lift and lubrication forces, and represent a key issue in modeling multiphase flows, due to the absence of good models for the complex interfacial phenomena. In this work the drag is the only interfacial force considered, expressed by

$$\overrightarrow{D_{12}} = \frac{3}{4}\frac{c_d}{d_2} r_2 \rho_1 \left|\overrightarrow{U_2} - \overrightarrow{U_1}\right| \left(\overrightarrow{U_2} - \overrightarrow{U_1}\right) \tag{5}$$

where d_2 is the droplet mean diameter and r_2 is the volume fraction of the second phase. The drag force acting on the droplets is given by the same expression, except for the volume fraction, which is for the air (r_1). The drag coefficient is given by the Shiller-Naumann correlation.

The turbulence modeling considers the κ-ε model for the airflow and a zero-equation model for the dispersed phase, where the eddy viscosity is assumed proportional to the continuum phase eddy viscosity.

The heat transfer problem is governed by the energy equation for multiphase flow, given by

$$\frac{\partial\left(r_i \rho_i c_{p,i} T_i\right)}{\partial t} + \vec{\nabla} \cdot \left(r_i \rho_i c_{p,i} \overrightarrow{U_i} T_i\right) = \vec{\nabla} \cdot \left[\left(r_i k_i + r_i c_{p,i} \frac{\mu_{t,i}}{\sigma_{t,i}}\right) \vec{\nabla} T_i\right] \quad (6)$$

where $c_{p,i}$, k_i, $\mu_{t,i}$ and $\sigma_{t,i}$ are the specific heat, conductivity, eddy viscosity and turbulent Prandl number for the phase i, respectively. There is no available relation for $\sigma_{t,i}$, so the value of 0.9 is usually adopted. In this work, it is assumed that the phases share the same temperature field, even though one can consider inter-phase heat transfer. Volume fraction conservation ($r_1 + r_2 = 1$) and the same pressure field for both phases ($p_1 = p_2 = p$) are the closure relations.

The boundary conditions include free-stream flow at the INLET boundary and prescribed pressure at the OUTLET boundary, as defined in Fig. 2. The free-stream value for the water volume fraction is obtained from the LWC (Liquid Water Content), which is an environmental condition. Both phases require the same kind of boundary conditions, except for the wall boundary where a special condition, known as the "degassing condition" must be applied. This condition considers the wall as an outlet for the dispersed phase while the continuous phase "sees" this boundary as a free-slip wall but with no mass through the wall.

Unfortunately, CFX does not support the correct boundary condition, which is a no-slip wall for the continuum phase and an *Outlet* for the dispersed phase. However, it was shown in early works that viscous and non-viscous air flow solutions produce quite close results.

Although many possibilities for turbulence models exist, it is recommended to use the k-ε model for the continuum phase and a zero-equation model for the dispersed phase in order to achieve good convergence and stability of the numerical solution.

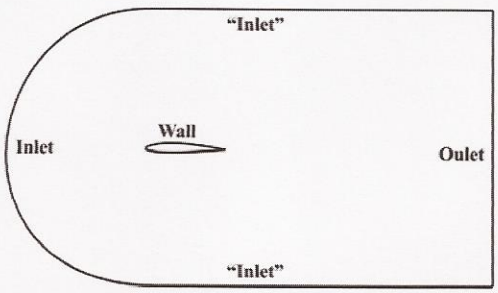

Fig. 2: Domain boundaries for application of the boundary conditions.

The collection efficiency in the Eulerian approach is computed directly from the external flow results. Since β is the ratio between the wall and free-stream water fluxes, according to Eq. (1), one has

$$\beta = -\frac{r_2 \overrightarrow{V_2} \cdot \vec{n}_{wall}}{r_{2,\infty}\rho_{2,\infty}\left|\overrightarrow{V_\infty}\right|} \qquad (7)$$

where $\vec{n}_{wall}$ is the unit normal vector at the wall (inward) and the sub-index 2 refers to water values.

THE THERMODYNAMIC MODEL

The amount of ice accumulated on the leading edge of an aerodynamic surface may be computed by a coupled energy-mass balance in control volumes defined over the external surface, as in the Messinger model (Messinger, 1953). In this work, the control volumes have the same length as the segments defining the external surface, and its thickness is equivalent to the thickness of water that would exist if no water were frozen, as in Fig. . 3.

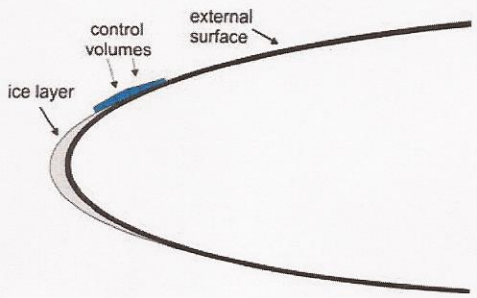

Fig. 3: Control volumes over the external surface.

The mass balance accounts for water impingement, evaporation, runback water and freezing, according to Fig. 4. The water droplets freeze immediately when impacting the surface, since they are in a meta-stable equilibrium state. Depending on the surface temperature and the total latent heat released due to freezing, a liquid film lies over the ice layer or the metallic surface. Then, part of this film can evaporate, flow over the surface (runback water) or freeze in a downstream position.

Balances begin at the control volumes adjacent to the stagnation point, where there is no runback water entering those control volumes, and follow toward the trailing edge through the upper and lower surfaces. The mass balance can be written as

$$\dot{m}''_{rb,in}\delta_s\Delta y + \dot{m}''_{imp}\Delta s\Delta y = \dot{m}''_{evap}\Delta s\Delta y + \dot{m}''_{freeze}\Delta s\Delta y + \dot{m}''_{rb,out}\delta_{s+\Delta s}\Delta y \qquad (8)$$

in which Δy is the dimension of the control volume in the span direction of the wing, for example. Since the model is two-dimensional, one can consider Δy equal to 1.

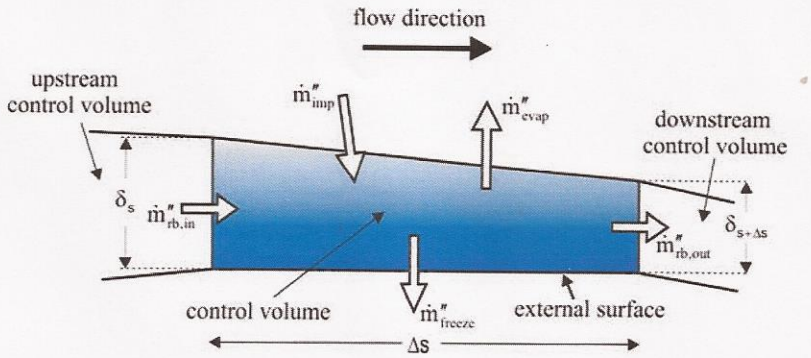

Fig. 4: Mass balance in a control volume.

The impingement flux is computed in terms of the collection efficiency as

$$\dot{m}''_{imp} = \beta \, LWC \, U_{\infty} \tag{9}$$

in which LWC is the liquid water content, which is an environment condition and is an input data for the model. More details about this term can be found in Silveira (2001), Silveira and Maliska (2001) and Wright (1995).

The freezing flux is computed by defining the freezing fraction, which is the fraction of water that freezes in the control volume and it is obtained from the enthalpy formulation for phase change problems, as

$$f_s = \frac{T_m + \Delta T_m - T}{2\Delta T_m} \tag{10}$$

in which T_m is the melting temperature of ice (273.15 K) and ΔT_m is a range around the melting temperature in which the water is assumed to freeze. Then, the freezing flux is given by

$$\dot{m}''_{freeze} = f_s \left(\dot{m}''_{imp} + \dot{m}''_{rb,in} \right) \tag{11}$$

Since there is no runback water entering the control volume adjacent to the stagnation point, the mass balance can be written for the runback flow leaving the control volume in the form

$$\dot{m}_{rb,out} = \dot{m}_{rb,in} + \left(\dot{m}''_{imp} - \dot{m}''_{evap} - \dot{m}''_{freeze} \right) \Delta s \tag{12}$$

The runback water leaving a control volume will be the runback water entering the next control volume. The film thickness and the film average velocity can be computed by assuming a linear velocity profile and applying zero velocity at the wall and momentum flux continuity at the interface with the external flow.

Some of the terms in the mass balance depend on the control volume temperature, which is assumed equal to the surface temperature. This temperature is obtained from an energy balance in the same control volume used for the mass balance, according to Fig. 5.

The energy balance accounts for sensible heat lost to the impinging droplets ($\dot{q}''_{s,imp}$), sensible heat transfer due to runback water ($\dot{q}''_{s,rb}$), kinetic heating from the airflow ($\dot{q}''_{ke,air}$), kinetic heating due to droplets impact ($\dot{q}''_{ke,water}$), convection heat losses ($\dot{q}''_{conv}$), evaporative cooling ($\dot{q}''_{evap}$), conduction into the metal or ice layer ($\dot{q}''_{cond}$) and latent heat released during solidification ($\dot{q}''_{lat}$).

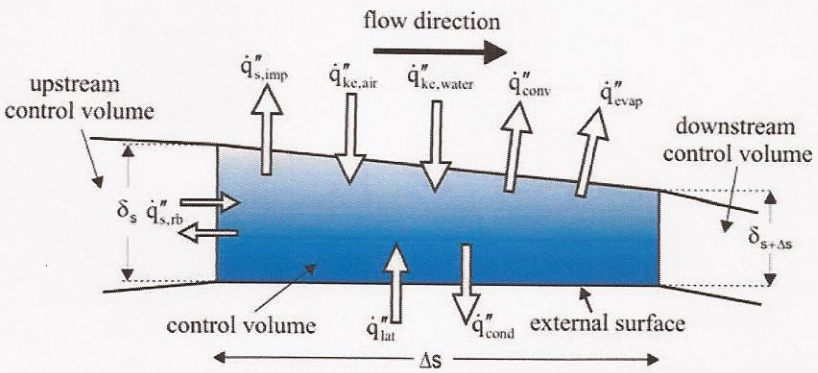

Fig. 5: Energy balance in the control volume.

Then, it can be written as

$$\dot{q}''_{ke,air}\Delta y\Delta s+\dot{q}''_{ke,water}\Delta y\Delta s+\dot{q}''_{lat}\Delta y\Delta s+\dot{q}''_{evap}\Delta y\Delta s+\dot{q}''_{cond}\Delta y\Delta s+\dot{q}''_{conv}\Delta y\Delta s+\dot{q}''_{s,imp}\Delta y\Delta s+\dot{q}''_{s,rb}\delta_s\Delta y=0 \quad (13)$$

After equating each of the fluxes as a function of the surface temperature, the energy equation is solved for this temperature by using an iterative method (Newton-Raphson in this work). In each iteration the mass balance is applied to account for the temperature influence in the mass transfer. The frozen mass in each segment, assuming that the freezing flux is constant in a time step, allows the calculation of the ice thickness by

$$\varepsilon_{ice}=\frac{\dot{m}''_{freeze}\Delta t}{\rho_{ice}} \quad (14)$$

The whole procedure consists of a) solve the external flow for the clean geometry, b) compute the ice thickness and the new profile geometry, c) solve again the external flow and add a new ice layer. The procedure is repeated

until the desired time level. A more detailed description of the thermodynamic model can be found in Silveira (2001), Silveira and Maliska (2001) and Wright (1995).

RESULTS

Tab. 1 summarizes the data for the simulated cases. For cases 1 to 3, the ice shapes provided by the two formulations are compared with experimental and simulated results provided by the Lewice code (Wright et. al (1997)). For cases 4 to 6, the ice profiles are compared with experimental data from Addy Jr. (2000). In the plots the results of this work are denoted by "Aeroicing Lagr." for the external flow solved with the Lagrangian formulation, and with "Aeroicing CFX", when it is done with the Eulerian approach. The first two cases are for rime ice, where there is no runback water and all of the water impinging the body freezes. The other cases are for glaze ice conditions, in which there is some runback water flowing over the surface, so that the thermodynamic behavior of the system is more complex. Only 3 cases are shown for space reasons.

Table 1: Summary of simulated cases.

Cases	**1**	**2**	**3**	**4**	**5**	**6**
Airfoil	NACA 0012	NACA 0012	NACA 0012	Business jet	Business jet	Business Jet
Chord(m)	0.5334	0.5334	0.5334	0.9144	0.9144	0.9144
AOA (°)	4	4	4	6	1.5	6
V_∞ (m/s)	58.1	93.8	58.1	90.02	128.61	90.02
T_∞ (K)	245.2	242.5	266.3	268.15	262.95	266.95
P_∞ (kN/m^2)	95.61	92.06	95.61	117.21	200.64	195.12
MVD (μm)	20	20	20	20	20	15
LWC (g/m^3)	1.3	1.05	1.3	0.54	0.54	1.0
Time (min)	8	6.2	8	6	6	15

Fig. 6 shows the results for the rime ice simulation (case 1). For this case, all of the water impinging the surface freezes, so that the mass balance reduces to the impingement and freezing fluxes. It can be seen that both methodologies for the external flow calculation produces equivalent results, since the ice shapes and ice accreted depend directly on the collection efficiency, which is being correctly calculated with both methodologies.

For cases 3 to 6, one has glaze ice conditions, in which part of the impinging water does not freeze and flows over the surface. The runback water may freeze at downstream positions, giving rise to the "ice horns".

Glaze ice occurs for free-stream temperatures closer to the phase change temperature and the heat transfer coefficient is very important in the heat balance. The results show that the Eulerian approach provides better ice shapes than the Lagrangian for these cases, as a consequence of a more accurate heat transfer coefficient calculation. These results are shown in Figs. 7 and 8.

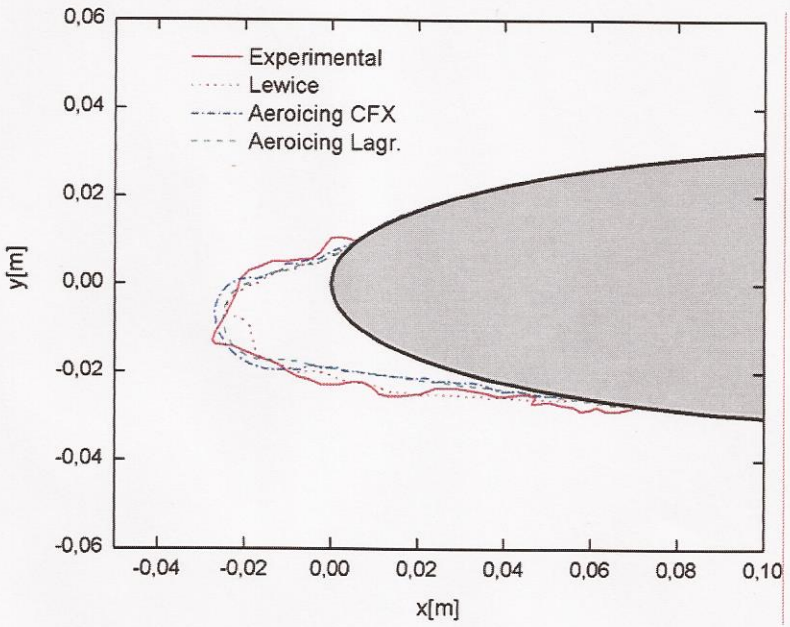

Fig. 6: Ice shapes results for case 1.

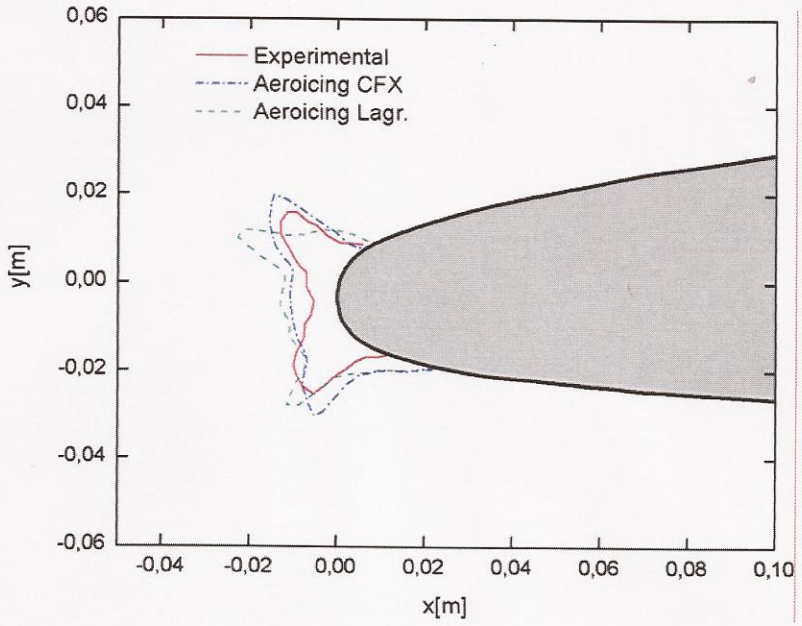

Fig. 7: Ice shapes results for case 5.

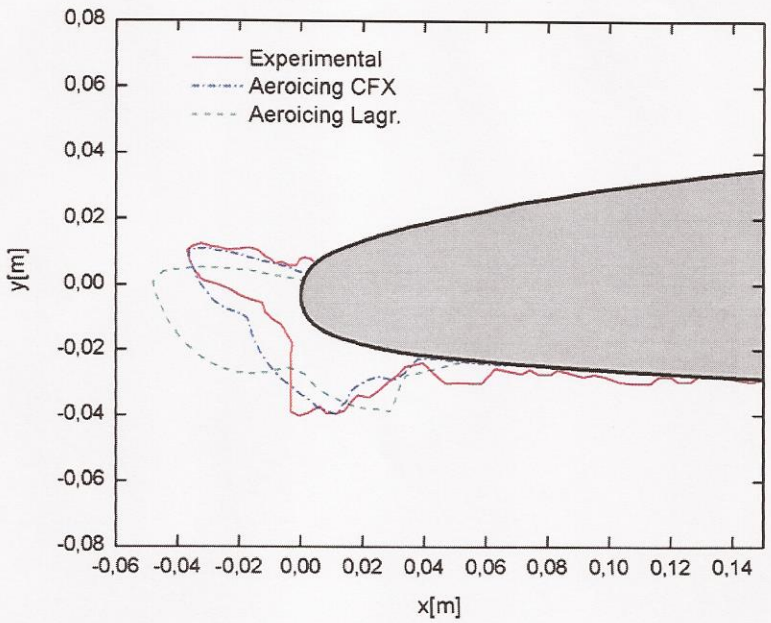

Fig. 8: Ice shapes results for case 6.

CONCLUDING REMARKS

This paper has shown the predictions of ice shapes obtained with two approaches for the external flow calculation. The results show that the Eulerian approach can provide better results in glaze ice conditions. However, the two-fluid model requires much more computational effort than a panel method with boundary layer integration and "particle-tracking" for simple 2D geometries. For 3D geometries, the Eulerian approach is more suitable, since the water mass flux impinging the surface is computed directly from the flow solution. In the case of the particle-tracking approach, the impingement position of each droplet must be computed, which is a very difficult process for complex geometries.

The boundary condition for the water droplets in the Eulerian approach (implemented in the CFX software), advanced in Silveira, et al. (2003) was successfully applied and can be still explored to yield even better results. The weak point of this formulation is the high computational cost, since one has to compute the airflow with a no-slip condition at wall, to obtain the shear stress , and then solve the two-phase flow to obtain the collection efficiency. Effort has been dedicated to change this boundary condition in the software to consider a no-slip slip wall condition for the continuous phase.

REFERENCES

Addy Jr., H.E., 2000, "Ice Accretion and Icing Effects for Modern Airfoils", NASA/TP 2000 – 210031.

Ansys Inc., 2003, "CFX 5.6 User´s Manual.

Bourgault, Y., Habashi, W. G., Dompierre, J. and Baruzzi, G.S., 1999, "A Finite Element Method Study of Eulerian Droplets Impingement Models", International Journal for Numerical Methods in Fluids, v. 29, pp. 429-449.

Gent, R.W. and Gent, R.W., 1994, "TRAJICE2 - A Combined Water Droplet Trajectory and Ice Accretion Prediction Code for Aerofoils," RAE-TR-90054.

Messinger, B.L., 1953, "Equilibrium Temperature of an Unheated Icing Surface as a Function of Air Speed". Journal of the Aeronautical Sciences, pp. 29-42.

Morency, F., Tesok, F. and Paraschivoiu, I., 1999, "Anti-Icing Simulation Using CANICE", Journal of Aircraft, v. 36, n. 6.

Naterer, G.F., 2002, "Multiphase Flow with Impinging droplets and Airstream Interaction at a Moving Gas/Solid Interface", International Journal of Multiphase Flow, v. 28, pp. 451-477.

Silveira, R. A., 2001, "Simulação Numérica da Formação de Gelo na Borda de Ataque de Perfis Aerodinâmicos", MSc Thesis, in Portuguese, Departamento de Engenharia Mecânica, Universidade Federal de Santa Catarina, Florianópolis, SC, Brasil.

Silveira, R. A., and Maliska, C.R., 2001, "Numerical Simulation of Ice Accretion on the Leading Edge of Aerodynamic Profiles", in Computational Heat and Mass Transfer-CHMT 2001, pp. 33-40, J. Pontes, Ed., E-Papers Publishing House Ltd., Rio de Janeiro.

Silveira, R. A., Maliska, C.R., Estivam, D.A. e Mendes, R., 2003, "Evaluation of Collection Efficiency Methods for Icing Analysis", Anais do XVII COBEM – International Congress of Mechanical Engineering, São Paulo – SP.

Wright, W. B., 1995, "Users Manual for the Improved NASA Lewis Ice Accretion Code Lewice 1.6", NASA CR – 198355.

Wright, W. B., Gent, R. W. and Guffond, D., 1997, "DRA/NASA/ONERA Collaboration on Icing Research Part II – Prediction of Airfoil Ice Accretion", NASA CR – 202349